

Nonequilibrium Screening of the Photorefractive Effect

D. D. Nolte and D. H. Olson

AT&T Bell Laboratories, Holmdel, New Jersey 07733

A. M. Glass

AT&T Bell Laboratories, Murray Hill, New Jersey 07974

(Received 8 March 1989)

The nonequilibrium occupation of multiple defect states in inhomogeneously illuminated crystals is demonstrated to have dramatic and previously unexpected consequences for the photorefractive behavior of electro-optic semiconductors. By using a simple screening formalism, we show for the first time that the standard photorefractive effect can be partially or entirely quenched. This nonequilibrium screening is observed in the thermally stimulated relaxation of diffraction efficiencies in four-wave mixing experiments performed on semi-insulating InP.

PACS numbers: 78.20.Wc, 71.55.Ht, 72.20.Jv

The photorefractive effect has gained considerable interest and importance because of applications in image processing,¹ optical phase conjugation,² and associative memory.³ The fundamental role of single defect levels in photorefractive crystals has long been recognized⁴ and full theoretical understanding has been achieved. In this Letter, we demonstrate that nonequilibrium charge stored in multiple defect levels can lead to dramatic modification of photorefractive behavior in ways that had not been previously recognized. We show for the first time that minority carriers trapped at defect sites can dynamically screen the internal space-charge fields generated by charge transferred in the dominant defect level. This results in a marked departure of the photorefractive behavior from that described by previous theoretical models. The theoretical framework used here emphasizes intuitive aspects of screening and yields considerable physical insight and simplicity over the use of cumbersome rate equations. For instance, one of the consequences of screening is a quenching of the photorefractive effect which we have observed experimentally at low temperatures in samples of semi-insulating Fe-doped InP. The strong sensitivity of nonequilibrium screening to microscopic defect properties (especially defect activation energies) raises the possibility of a new spectroscopy of defects in semi-insulating materials. Furthermore, this new understanding of nonequilibrium screening will lead to better control and optimization of photorefractive materials.

Many aspects of the photorefractive effect have been understood through the "standard model" in which a single deep level pins the Fermi level nearly midgap.⁵ In the four-wave mixing geometry, two coherent pump laser beams interfere coherently inside the semi-insulating sample, generating a volume holographic grating. Within the regions of constructive interference photoexcitation of both electrons and holes is possible.⁶ The carriers diffuse or drift to the dark regions and are re-

trapped by the deep level (see Fig. 1). This charge transport produces internal space-charge fields which modify the index of refraction of the material through the electro-optic effect. The resulting index grating is probed by a third laser beam, and the magnitude of the holographic grating is measured as the diffracted intensity of the probe beam. The diffraction efficiency η is proportional to the square amplitude of the modulated space-charge field, $\eta = \sin^2(cE)$, where the constant c depends on the sample geometry.

At finite temperatures, the internal electric fields, modulated by the light intensity, have contributions from diffusion ($E_D = k_B TK/e$) as well as from drift in an external applied field E_0 . $K = 2\pi/\Lambda$ is the spatial frequency and Λ is the grating spacing. The internal modulated space-charge field when a single photocarrier dominates is given by⁷

$$E_{sc} = \frac{(E_0 + iE_D)E_{max}}{E_{max} + E_D - iE_0} \frac{m}{1 + \sigma_d/\sigma_0} \quad (1)$$

for an intensity modulation of $I = I_0[1 + m \sin(Kx)]$, where m is the modulation index. The dark and photoconductivities are given by σ_d and σ_0 the space-charge

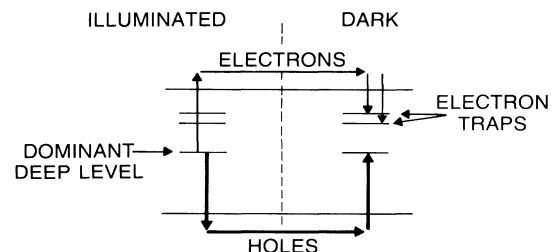


FIG. 1. Schematic depiction of nonequilibrium screening of the photorefractive effect. The trapped minority electrons will redistribute to screen the electric field built up by the charge transfer within the dominant defect level.

field is limited to the saturation value

$$E_{\max} = eN_{\text{eff}}/\epsilon\epsilon_0K, \quad (2)$$

where $N_{\text{eff}} = f_1(1-f_1)N_1$ is the maximum space-charge density that can be transferred with a total concentration N_1 of defects with equilibrium filling factor f_1 depending on the initial compensation of the material. As seen from Eqs. (1) and (2), the photorefractive effect in the standard model depends only on the macroscopic properties of the material, such as the dielectric constant, and on macroscopic properties of the defects, such as their total concentration and compensation. The temperature dependence at low temperature originates only from the diffusion of free carriers. At high temperature, the dark conductivity overcomes the photoconductivity, and the photorefractive effect is reduced by the dielectric relaxation of the free carriers.

When additional defect levels are present (which is usually the case in practice), these defect levels can also trap the photoexcited carriers. The charge trapped in these defects will be acted upon by the electric fields set up by the transfer of charge in the dominant deep level and the spatial distribution of this additional trapped charge will alter in a self-consistent manner. If the additional defects trap the minority carriers, then the minority carriers will redistribute to cancel the fields built up by the majority carrier. Any reservoir of charge that can redistribute in response to a local potential will, of course, lead to screening. The nonequilibrium charge trapped in the minority defect states is such a reservoir of charge, provided that these can redistribute. Although the trapped charge on the defects is immobile in the dark, during illumination the charge is able to adjust to the electric fields by photoionization and recapture.

As an example, we consider the general case of a crystal having a total concentration N_1 of midgap defects which pin the Fermi level. Photoexcitation of both electrons and holes occurs from this dominant deep level. We assume additional defect levels are also present with concentration N_i but with energies shallower than the dominant defect energy. To illustrate the effects of screening, we treat the more specific situation in which the photocarrier density from the dominant defect is predominantly holes, and the additional defect levels trap only the electrons as shown in Fig. 1. This problem can be approached, in principle, through the solution of the coupled differential equations governing the various emission and capture rates. In practice, however, this problem becomes intractable for more than even one minority trap.⁷ In our simple screening approach, we include the general case of an applied field and multiple minority-carrier traps for all temperatures, but neglect bipolar conductivity. The effects of bipolar conductivity are well understood.⁶ The nonequilibrium occupation of the electron trap is given by

$$\frac{N_i^-}{N_i^0} = \frac{\sigma_i s_1}{\sigma_1(s_i + e_i/I_0)} \frac{N_1^-}{N_1^0}, \quad (3)$$

where σ_1 and σ_i are the electron (minority-carrier) capture cross sections of the dominant deep level and the minority traps, respectively. The electron photoionization cross sections are given by s_1 and s_i . The charge states for all defects are assumed to be negative or neutral $(-,0)$. The thermal emission rate of trapped carriers from the electron trap is $e_i = \sigma_i N v \exp(-E_i/k_B T)$, where E_i is the defect binding energy, v is the thermal velocity of free carriers, and N is the effective density of states. An important feature of Eq. (3) is the strong temperature dependence of the thermal emission rate. The maximum charge that can be transferred in the electron trap is

$$n_i = f_i(1-f_i)N_i = \frac{N_i^0 N_i^-}{N_i}, \quad (4)$$

with filling factor f_i under homogeneous illumination. The value n_i represents a nonequilibrium reservoir of charge that has been built up under the illumination of the pump laser. This charge is available to screen the field in Eq. (1). Maximum screening occurs when the minority defect level is exactly half occupied, accommodating the maximum transfer of charge between the illuminated and dark defect levels in the crystal.

In the familiar case of screening by free carriers, the effect of screening is calculated by determining how a local potential alters the local carrier density. Because the coherent interference of plane-wave pump beams leads to sinusoidal variation of light intensity, we consider the screening of a sinusoidal field, $E^0(x) = E_0 \sin(Kx)$. The expression for the screened internal electric field in this case is

$$E_{\text{int}}(x) = \frac{E^0(x)}{1 + k_s^2/K^2}, \quad (5)$$

where k_s is the Debye screening wave number given by

$$k_s^2 = \frac{e^2(n_2 + n_3 + \dots)}{\epsilon\epsilon_0 k_B T}. \quad (6)$$

The concentrations n_i are the charge in the multiple minority traps given by Eq. (4) that are available for screening.

The nonequilibrium screening reduces the electric field per hole transferred within the dominant deep level. Therefore, to build up an internal space-charge field that counteracts the applied or diffusion fields, more holes must be transferred to develop the same magnitude electric field. If the screening is large, then the transfer of holes quickly saturates, limiting the space-charge field to a value less than E_{\max} [Eq. (2)]. The space-charge field, including the nonequilibrium screening, is now given by

$$E_{\text{sc}} = \frac{(E_0 + iE_D)E_{\max}}{E_{\max} + (1 + k_s^2/K^2)(E_D - iE_0)} \frac{m}{1 + \sigma_d/\sigma_0}. \quad (7)$$

At small fields (E_0 or E_D) or small screening, the space-charge field reduces to Eq. (1). However, at large fields

or large screening, the product in the denominator involving the screening term will dominate, and the space-charge field will saturate at the reduced field $E_{\max}/(1+k_s^2/K^2)$. If the minority-carrier trap density is comparable to or larger than N_{eff} of the dominant deep level, then the screening of the photorefractive effect may be substantial. A strong temperature dependence is expected for the screening because of the temperature dependence of the thermal emission rates e_i from the minority-carrier traps which appear in Eq. (3). At sufficiently high temperatures, the thermal ionization rate of the electron trap is much larger than the capture rate, and insufficient charge will be trapped in the defect level to screen the internal fields.

We have observed nonequilibrium screening of the photorefractive effect in four-wave mixing experiments performed on two Fe-doped semi-insulating InP samples having resistivities (300 K) of 10^8 and 10^6 Ω cm cut from the tail and the seed ends of the boule, respectively. Volume holograms were written in the InP crystals by pump beams originating from a cw Nd-doped yttrium aluminum garnet (YAIG:Nd) laser at a wavelength of 1.06 μm . A probe beam originating from a second YAIG:Nd laser with a wavelength of 1.32 μm was used to measure the diffraction efficiency of the index grating written by the pump beams. The grating amplitude was measured by chopping one of the pump beams or by chopping the probe beam, and the diffracted probe signal was detected by an InGaAs photodiode and a lock-in amplifier. Qualitatively similar data were obtained for both chopping modes, indicating that our chopping frequency was sufficiently slow compared with the response rate of the grating decay for all temperatures. The thermal measurements were obtained by placing the

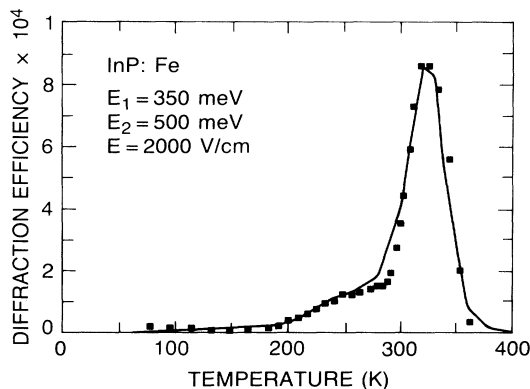


FIG. 2. Diffraction efficiency as a function of temperature for InP:Fe. The experimental data were taken with an applied field of 2000 V/cm at a chopping frequency of 100 Hz. The solid curve is the result of Eq. (7) fitted to the experimental data by assuming two defects occur in the material with concentrations equal to 5 times the Fe impurity concentrations: one with a binding energy of 350 meV, the other with a binding energy of 500 meV.

sample in a Janis supervaritemp cryostat. This allowed close control of cooling and heating rates. The grating spacing in the material for these experiments was 3.4 μm .

The temperature dependence of the diffraction efficiency from InP:Fe sample no. 1 (10^8 Ω cm) is shown in Fig. 2 for an applied field of 2000 V/cm and a chopping frequency of 100 Hz. Data from sample no. 2 (10^6 Ω cm) for an applied field of 1000 V/cm are shown in Fig. 3 compared with the standard model. The pump laser power was 40 mW/cm² in each beam, and the probe beam power was sufficiently small so that no erasure of the diffraction gratings occurred during read-out. The diffraction efficiency exhibits a marked temperature dependence. Below 160 K, the signal is entirely quenched. A shoulder is present between 160 and 270 K before the diffraction efficiency greatly increases near room temperature, with a peak slightly above room temperature. While the high-temperature decrease is expected from the dielectric relaxation from the dark conductivity, the low-temperature dependence of the diffraction efficiency from this InP sample is in sharp disagreement with the prediction from the standard model of the photorefractive effect. The results of the standard model are compared with our data from sample no. 2 in Fig. 3. At low temperature in the standard model, the diffraction efficiency (with an applied field) is nearly independent of temperature, depending only on the value of the applied field. At temperatures near room temperature, the diffraction efficiency increases slightly, caused by the addition of the diffusion field to the drift field. The radical deviation of the experimental data from the standard model can now be understood in terms of the nonequilibrium screening model involving two minority trap levels. The results of Eq. (7) are compared with experiment in Figs. 2 and 3. An excellent fit to the data is obtained using binding energies of 350 and 500 meV for the two defects, with concentrations of 5

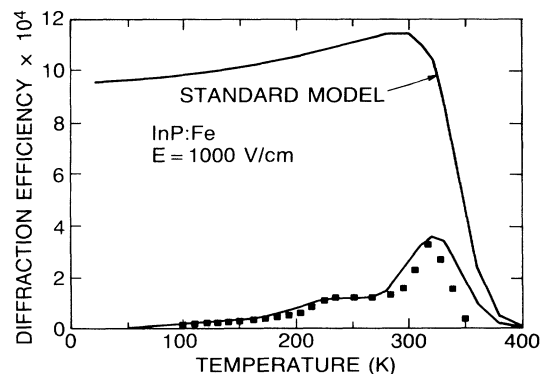


FIG. 3. Comparison of the standard model from Eq. (1) with the data from sample no. 2 and the fit from Eq. (7) for an applied field of 1000 V/cm. This sample has lower resistivity and less screening than the sample in Fig. 2.

and 1 times N_{eff} for samples no. 1 and no. 2, respectively. Other parameters of these defects, such as the cross sections, for simplicity are taken to be equal to the values for the Fe level although the results are insensitive to these parameters. The defect energies chosen to fit the diffraction data match closely with the energy levels of the configurationally bistable $M\text{Fe}$ centers that are known to occur in high concentration in conducting Fe-doped InP.⁸

It is interesting to note that earlier photorefractive studies of InP:Fe⁹ at room temperature occurred fortuitously near the peak response of this material. Indeed, it might be expected that screening effects of this kind may have affected earlier studies even of wide-gap electro-optic materials. This nonequilibrium screening is, in fact, reminiscent of the fixing of holograms at elevated temperatures in LiNbO₃. In this case, dynamic screening occurs via ionic space-charge drift during recording instead of by minority traps as in the present case.¹⁰

In conclusion, we have shown that the nonequilibrium occupation of minority-carrier traps during the writing of holographic gratings in electro-optic crystals can lead to essentially complete screening of the photorefractive effect. The screening formulation of this problem is simple and physically intuitive and experimental confirmation of this behavior has been observed in InP:Fe. The sensitivity of this effect to defect properties, especially the activation energy, raises the prospect of a new spectroscopy of defects in semi-insulating material. In

addition, the new understanding of nonequilibrium screening should have considerable impact on the design of photorefractive materials and on the interpretation of their properties.

¹J. Feinberg, Phys. Today **41**, No. 10, 46 (1988), and references therein.

²J. P. Huignard, J. P. Herriau, P. Aubourg, and E. Spitz, Opt. Lett. **4**, 21 (1979).

³D. Z. Anderson, Mater. Res. Bull. **13**, 30 (1988), and references therein.

⁴F. S. Chen, J. Appl. Phys. **40**, 3389 (1969); G. E. Peterson, A. M. Glass, and T. J. Negran, Appl. Phys. Lett. **19**, 130 (1971); J. J. Amodei, Appl. Phys. Lett. **18**, 22 (1971).

⁵N. V. Kukhtarev, Pis'ma Zh. Tekh. Fiz. **2**, 1114 (1976) [Sov. Tech. Phys. Lett. **2**, 438 (1976)]; M. G. Moharam, T. K. Gaylord, and R. Magnusson, J. Appl. Phys. **50**, 5642 (1979); G. C. Valley and J. F. Lam, in *Photorefractive Materials and Their Applications*, edited by P. Gunter and J.-P. Huignard (Springer-Verlag, Berlin, 1988).

⁶S. Ducharme and J. Feinberg, J. Opt. Soc. Am. B **3**, 283 (1986); E. P. Strohkendl, J. M. C. Jonathan, and R. W. Hellwarth, Opt. Lett. **11**, 312 (1986).

⁷G. C. Valley, J. Appl. Phys. **59**, 3363 (1986).

⁸M. Levinson, M. Stavola, P. Besomi, and W. A. Bonner, Phys. Rev. B **30**, 5817 (1984).

⁹A. M. Glass, A. M. Johnson, D. H. Olson, W. Simpson, and A. A. Ballman, Appl. Phys. Lett. **44**, 948 (1984).

¹⁰D. L. Stabler and J. J. Amodei, Ferroelectrics **3**, 107 (1972).